Homoserine Dehydrogenase of *Escherichia coli* K 12λ. I. Feedback Inhibition by L-Threonine and Activation by Potassium Ions*

James W. Ogilvie,† James H. Sightler,‡ and Richard B. Clark

ABSTRACT: The isolation of homoserine dehydrogenase from *Escherichia coli* K 12λ is described and the results of a detailed study of the homoserine dehydrogenase catalyzed oxidation of L-homoserine to aspartic β-semialdehyde at pH 8.9 are presented. Based on the results of the kinetic study, a tentative two-substrate–two-modifier model is proposed which appears to be consistent with the experimental data, including that for the activation of the enzyme by K^+ and the inhibition of the enzyme by L-threonine. The salient features of the tentative model are (1) the activation of the enzyme by K^+ is essential and involves two highly cooperative K^+ binding sites, (2) the activation of the enzyme by K^+ must precede the binding of homoserine by the enzyme, and (3) both the K^+-activated enzyme–nicotinamide–adenine dinucleotide phosphate–homoserine complex and the K^+-activated enzyme–nicotinamide–adenine dinucleotide phosphate–homoserine–threonine complex are capable of forming products. An initial velocity equation is derived by a rapid equilibrium treatment of the model and the estimated values of all of the enzyme–ligand dissociation constants are presented.

In recent years a number of models, some more general than others, have been proposed to explain the kinetics and properties of regulatory enzymes (Frieden, 1964, 1967; Monod *et al.*, 1965; Koshland *et al.*, 1966; Rabin, 1967; Sweeny and Fisher, 1968), and the kinetics and properties of a few specific regulatory enzymes have been rationalized in terms of individual models (Frieden, 1963; Atkinson *et al.*, 1965; Sanwal *et al.*, 1965; Ferdinand, 1966; Kirschner *et al.*, 1966; Frieden and Colman, 1967; Changeux and Rubin, 1968). In the hope that the latter approach, the rationalization of the kinetic behavior of specific regulatory enzymes in terms of individual models, might ultimately lead to some generalizations about the mechanisms employed by these enzymes, we initiated an investigation of the kinetics of homoserine dehydrogenase I of *Escherichia coli* K 12.

Homoserine dehydrogenase, an enzyme which catalyzes the reaction L-aspartic β-semialdehyde + NADPH + H^+ ⇌ L-homoserine + $NADP^+$, occupies a key position between branch points in the biosynthetic pathway responsible for the conversion of aspartic acid to lysine, threonine, isoleucine, and methionine in a number of microorganisms. It has been clearly established that homoserine dehydrogenase I in *E. coli* K 12 Hfr H is subject to both feedback inhibition and repression by L-threonine, one of the end products of the pathway, as well as to an activation by potassium ions which is antagonized by sodium ions (Patte *et al.*, 1963). Another intriguing property of the enzyme is its close physical association with the protein which carries one of the aspartokinase activities (Patte *et al.*, 1966). The particular aspartokinase with which the homoserine dehydrogenase I is associated is also subject to feedback inhibition by L-threonine.

Homoserine dehydrogenase I from *E. coli* K 12 was selected for the present investigation because the enzyme possesses the interesting properties outlined above, and because the kinetic behavior of the enzyme appears to be relatively straightforward, with no indication of cooperative homotropic interactions of either substrate (Patte *et al.*, 1963). In this latter respect, the homoserine dehydrogenase of *E. coli* differs markedly from the homoserine dehydrogenase of *Rhodospirillum rubrum* (Datta and Gest, 1965). The results of the investigation which are reported herein pertain almost entirely to the reaction in the reverse direction, *i.e.*, the catalysis of the oxidation of L-homoserine to aspartic β-semialdehyde with the concomitant reduction of $NADP^+$. A model which appears to be consistent with the experimental data, including that for K^+ activation and threonine inhibition, is presented. A preliminary report of some of the results of this investigation has appeared (Ogilvie and Sightler, 1968).

Materials and Methods

Materials. L-Threonine (*allo* free), DL-allylglycine, and streptomycin sulfate were obtained from Nutritional Biochemicals. DL-Homoserine was a product of Mann. Isocitrate dehydrogenase, DL-isocitrate, thiamine hydrochloride, and $NADP^+$ were obtained from Sigma. Sephadex G-25 and G-200 and Sepharose 4B were products of Pharmacia. DEAE-cellulose was a product of Schleicher & Schuell and was purified by the procedure of Peterson and Sober (1956). Acrylamide, *N,N'*-methylenebisacrylamide, and *N,N,N',N'*-tetramethylethylenediamine were obtained from Eastman. Aspartic β-semialdehyde was prepared by the method of Black and

* From the Department of Physiological Chemistry, The Johns Hopkins School of Medicine, Baltimore, Maryland, and the Department of Biochemistry, University of Virginia, School of Medicine, Charlottesville, Virginia. *Received January 20, 1969.* Supported by research grants from the National Institutes of Health (H-4977, GM16917) and the National Science Foundation (GB 6894).

† Present address: Department of Biochemistry, University of Virginia, School of Medicine, Charlottesville, Virginia 22901.

‡ Taken in part from a thesis to be submitted by J. H. S. to The Johns Hopkins University in partial fulfillment of the requirements for the degree of Doctor of Philosophy.

TABLE I: Purification of Homoserine Dehydrogenase of *E. coli* K 12λ.

Fraction	Total Vol (ml)	Protein Concn (mg/ml)	Total Enzymatic Act.[a] (units)	Sp Act. (units/mg)	Recov[b] (%)
I (crude extract)	164	25	690	0.168	(100)
II (second 30–45% $(NH_4)_2SO_4$ fraction)	10.28	56.1	748	1.30	108[c]
III (DEAE fraction)	13	3.25	350	8.28	51
IV (Sepharose fraction)	2	1.1	136	61.8	20

[a] Enzymatic activity based on assay in the forward direction, *i.e.*, L-aspartic β-semialdehyde + NADPH + H^+ → $NADP^+$ + L-homoserine. Initial conditions: 250 mM potassium phosphate (pH 7.6), 130 μM NADPH, 2 mM DL-aspartic β-semialdehyde, and 33 μM L-threonine in a total volume of 3.0 ml at 27°. A unit of activity is that amount of enzyme which will oxidize 1 μmole of NADPH/min under the conditions specified above. [b] Recovery based on the enzymatic activity present in the crude extract. [c] Recovery at this stage of purification is typically slightly greater than 100%. The explanation for this is unknown.

Wright (1955) and NADPH was prepared according to the procedure described by Evans and Nason (1953). The culture of *E. coli* K 12λ was a gift of Dr. Gunther von Ehrenstein. All other chemicals were obtained from commercial sources and were reagent grade.

Growth of E. coli K 12λ. The bacteria were grown on medium 63 of Cohen and Rickenberg (1956) at 37° with aeration. The cells were harvested in the late log phase of growth, washed with 10 mM potassium phosphate (pH 7.6) containing 100 μM EDTA, and the packed cells were stored at −15°.

Enzyme Purification. All purification procedures were performed at 0–5° unless specifically stated otherwise. Buffer A refers to 10 mM potassium phosphate (pH 7.6) containing 10 mM L-threonine and 100 μM EDTA. Buffer B refers to 10 mM potassium phosphate (pH 7.6) containing 5 mM L-threonine, 100 μM dithiothreitol, and 100 μM EDTA. Buffer C refers to buffer B containing 500 mM KCl.

The thawed cells were suspended in three volumes of buffer A and disrupted sonically in a 20-kc MSE sonicator for 10 min. After centrifugation at 20,000*g* for 20 min, the supernatant fraction was decanted and labeled fraction I (crude extract). A quantity of streptomycin sulfate sufficient to give a final concentration of 17.5 mg/ml of I was slowly added to I with gentle stirring, and the stirring was continued for 1 hr after completion of the addition. The resulting precipitate was removed by centrifugation and the supernatant fraction was brought to 30% saturation in $(NH_4)_2SO_4$ by the slow addition of $(NH_4)_2SO_4$. After standing for 30 min, the precipitate was removed by centrifugation and the supernatant fraction was adjusted to 45% saturation in $(NH_4)_2SO_4$. After standing for 1 hr, the precipitate was collected by centrifugation and dissolved in a volume of buffer A equivalent to the initial volume of fraction I. The entire $(NH_4)_2SO_4$ fractionation procedure was repeated exactly as described for the first $(NH_4)_2SO_4$ fractionation with the single exception that the protein precipitating between 30 and 45% saturation with $(NH_4)_2SO_4$ was dissolved in a volume of buffer A equivalent to one-tenth the initial volume of fraction I. Contaminating $(NH_4)_2SO_4$ in the second 30–45% $(NH_4)_2SO_4$ fraction was removed by gel filtration on a Sephadex G-25 column equilibrated with buffer A, and the eluate containing the $(NH_4)_2SO_4$-free protein fraction was concentrated by pressure dialysis to a protein concentration of 40 mg/ml. This fraction was labeled fraction II (second 30–45% $(NH_4)_2SO_4$ fraction) and stored at −15°.

A sample of fraction II containing 200 mg of protein in buffer A was placed on a DEAE-cellulose column (3 × 54 cm) which had been packed under 2-psi air pressure with a slurry of DEAE-cellulose in buffer B. The column was developed at room temperature with 6 l. of a linear gradient of 0.05–0.5 M KCl in buffer B, and the eluate was collected in 5-ml fractions in a refrigerated fraction collector at 4°. The fractions were assayed for enzymatic activity and the fractions of highest specific activity were pooled and the protein was precipitated by the addition of 0.36 g of $(NH_4)_2SO_4$/ml of the pooled fraction. The precipitated protein was isolated by centrifugation and redissolved in a sufficient quantity of buffer B to yield a protein concentration of 10 mg/ml. This fraction was labeled fraction III (DEAE fraction) and stored at −15°.

A 4-ml sample of fraction III containing 40 mg of protein was placed on a jacketed Sepharose 4B column (2.5 × 80 cm) which had been packed with a slurry of Sepharose 4B in buffer C. The column, maintained at 4°, was eluted with buffer C, and the fractions containing enzyme of highest specific activity were combined. The protein in the combined fraction was precipitated by the addition of 0.36 g of $(NH_4)_2SO_4$/ml of the fraction and isolated by centrifugation. The isolated protein, labeled fraction IV (Sepharose fraction), was dissolved in buffer B (1 mg of protein/ml) and stored at −15°.

A summary of the purification procedure is presented in Table I. Protein in fraction I was estimated by the microbiuret method (Zamenhof, 1957); protein in the other fractions was estimated spectrophotometrically (Warburg and Christian, 1941).

Enzyme Assay. Homoserine dehydrogenase activity was assayed by following the change in NADPH concentration spectrophotometrically at 340 mμ with a Beckman DU spectrophotometer equipped with a Sargent SRL recorder and a cell compartment thermostated at 27°. Assays were performed in cuvets with a 1-cm light path employing reaction mixtures with a final volume of 3 ml. All of the rates were linear with time for at least 45 sec and the initial velocity was determined from the linear portion of the rate curve. The initial velocity of the reaction measured in the forward direction or in the reverse direction was proportional to the enzyme concentration

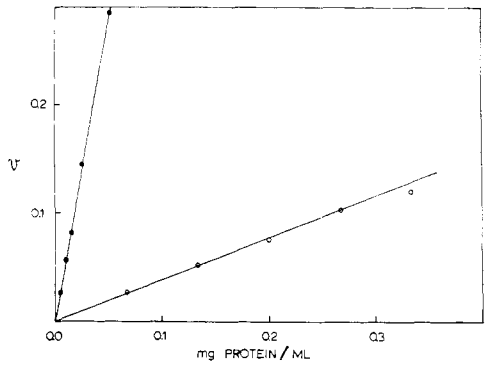

FIGURE 1: Effect of enzyme concentration on the initial reaction velocity measured in the forward (●) and reverse (⊙) directions at 27°. Initial conditions, forward direction assay (L-aspartate β-semialdehyde ⟶ L-homoserine): 0.1 M Tris-HCl (pH 7.6), 33 μM L-threonine, 0.4 M KCl, 130 μM NADPH, and 1.88 mM DL-aspartate β-semialdehyde. Initial velocity expressed as −Δ absorbance per minute at 340 mμ. Initial conditions, reverse direction assay (L-homoserine ⟶ L-aspartate β-semialdehyde): 0.1 M Tris-HCl (pH 8.95), 33 μM L-threonine, 0.8 M KCl, 320 μM $NADP^+$, and 25 mM DL-homoserine. Initial velocity expressed as Δ absorbance per minute at 340 mμ.

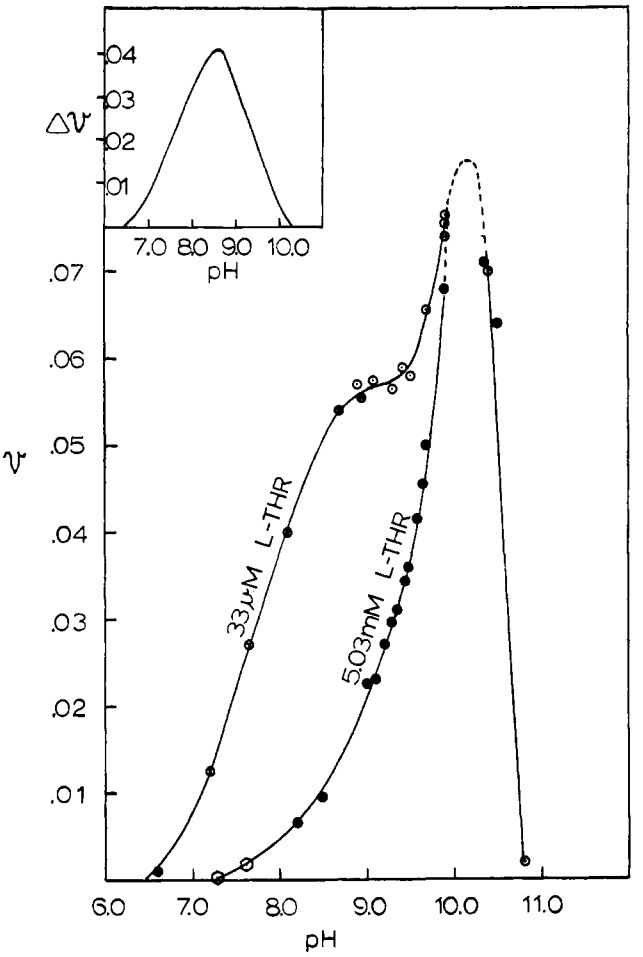

FIGURE 2: Effect of L-threonine concentration on the pH–activity curve for the homoserine dehydrogenase catalyzed oxidation of homoserine. Initial conditions: 25 mM DL-homoserine, 309 μM $NADP^+$, 0.4 M KCl, and either 0.1 M Tris-HCl plus 33 μM L-threonine (⊗), 0.1 M potassium glycinate plus 33 μM L-threonine (⊙), 0.1 M Tris-HCl plus 5.03 mM L-threonine (○), or 0.1 M potassium glycinate plus 5.03 mM L-threonine (●). Inset: a difference curve derived by subtracting the pH–activity curve at 5.03 mM L-threonine from the pH–activity curve at 33 μM L-threonine. Initial velocity expressed as Δ absorbance per minute at 340 mμ.

(Figure 1). Fraction II, the enzyme preparation employed in all of the kinetics studies, contained 40 mg of protein/ml and was stable for months when stored at −15° in the presence of 10 mM L-threonine. A 10-μl aliquot of fraction II was used in each kinetic experiment when the reaction was investigated in the reverse direction; therefore, the final concentration of protein and the minimum concentration of L-threonine present in the reaction mixture in each reverse direction assay was 133 μg/ml and 33 μM, respectively. DL-Homoserine was used in all reverse direction assays; however, since D-homoserine is neither a substrate nor an inhibitor of the enzyme (Patte *et al.*, 1963), the double-reciprocal plots and the calculation of the kinetic parameters are based on the concentration of L-homoserine only.

Disc Electrophoresis. The procedure of Davis (1964) as modified by Davis *et al.* (1967) was employed with the additional modifications that (A) the small pore gel was buffered with 88 mM Tris-HCl (pH 7.9) containing 10 mM L-threonine, (B) the large pore gel was buffered with 27.6 mM imidazole-HCl (pH 6.0) containing 10 mM L-threonine, (C) the sample was applied in 0.3 ml of 100 mM imidazole-HCl buffer (pH 6.0) containing 5 mM L-threonine, 500 μM dithiothreitol, and 30% sucrose, and (D) the reservoir buffer was 30 mM asparagine, adjusted to pH 7.3 with Tris, containing 5 mM L-threonine, 500 μM dithiothreitol, and 1 ml of 0.02% bromophenol blue per l. The electrophoresis was conducted at a constant current of 4 mA/tube at 4° until the bromophenol blue had migrated 4.5 cm into the gel. The gels were removed from the tubes and either stained for protein by immersing the gel in 7% acetic acid containing 1% Buffalo Black NBR for 1 hr or stained for homoserine dehydrogenase activity by incubating the gel at 37° for 10 min in a solution containing 50 mM L-homoserine, 1 mM $NADP^+$, 100 mM Tris-HCl (pH 8.9), 400 mM KCl, 0.25 mg of nitrotetrazolium blue/ml, and 0.025 mg of phenazine methosulfate/ml. The gels stained for protein were destained by placing them in 7% acetic acid for 48 hr. The gels stained for homoserine dehydrogenase activity were rinsed with H_2O, fixed in 7% acetic acid, and stored in H_2O. Gels stained for protein or for homoserine dehydrogenase activity were scanned at 620 mμ in a Gilford Model 240 spectrophotometer equipped with the 2410 linear transport.

Results

The enzyme preparation employed throughout this investigation was fraction II. Thus far, the kinetic properties of fraction II appear to be identical with those of the more recently obtained and more highly purified preparations, fractions III and IV. The pH–rate profiles for the fraction II catalyzed oxidation of L-homoserine by $NADP^+$ in the presence of a high concentration (5 mM) and a low concentration (33 μM) of the inhibitor L-threonine are presented in Figure 2. Homoserine dehydrogenase is stabilized by threonine; thus, the stock enzyme solution routinely contained 10 mM L-threonine, and the low concentration of 33 μM L-threonine in the assay system re-

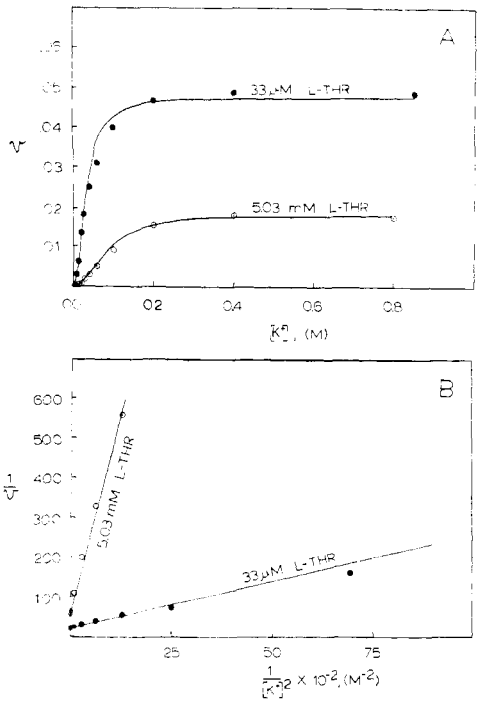

FIGURE 3: Effect of potassium ion concentration on the initial reaction velocity. (A) Plot of v *vs.* $[K^+]$. Initial assay conditions: 0.1 M Tris-HCl (pH 8.8), 310 μM $NADP^+$, 25 mM DL-homoserine, and either 33 μM L-threonine (●) or 5.03 mM L-threonine (⊙). Initial velocity expressed as Δ absorbance per minute at 340 mμ. Solid lines: theoretical curves calculated from eq 1. (B) The data of part A plotted in the double-reciprocal form, $1/v$ *vs.* $1/[K^+]^2$. ● = 33 μM L-threonine; ○ = 5.03 mM L-threonine. Solid lines: theoretical curves calculated from eq 1.

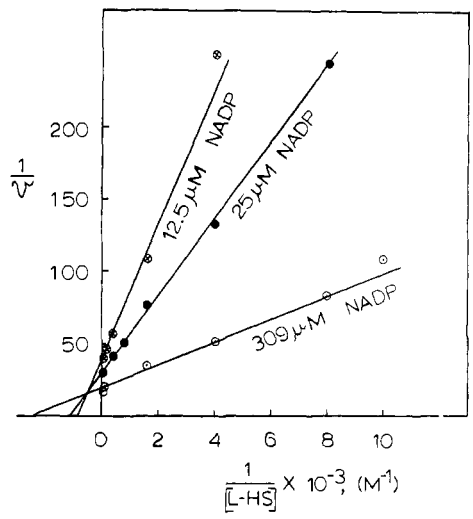

FIGURE 4: Double-reciprocal plots of initial reaction velocity *vs.* homoserine concentration at three different initial concentrations of $NADP^+$. Initial assay conditions: 0.1 M Tris-HCl (pH 9.1), 0.4 M KCl, 33 μM L-threonine, and either 309 μM $NADP^+$ (⊙), 25 μM $NADP^+$ (●), or 12.5 μM $NADP^+$ (⊗). Initial velocity expressed as Δ absorbance per minute at 340 mμ. Solid lines: theoretical curves calculated from eq 1.

sulted from the dilution of the stock enzyme solution in the assay procedure. As a first approximation, assays performed at 33 μM L-threonine were considered to be in the virtual absence of threonine since this concentration of threonine was observed to have very little effect on the catalytic activity of the enzyme. The pH–rate profile obtained at the low concentration of threonine is unusual in that it appears to possess a shoulder in the vicinity of pH 9; however, it should be pointed out that the data above pH 9.5 are less reliable and less complete because of an apparent increase in the lability of the enzyme above pH 9.5. From Figure 2 it can also be seen that the inhibitory effect of a fixed concentration of L-threonine is very pH dependent, with 5 mM L-threonine producing total inhibition in the vicinity of pH 7.0, approximately 65% inhibition in the vicinity of pH 9.0, and essentially no inhibition above pH 10. At pH 9.0, a threonine concentration of 5 mM is approaching the saturating concentration even though the inhibition produced is far from complete. The saturating concentration of L-threonine at other pH values has not yet been determined. All subsequent kinetic experiments were performed at pH 8.8–9.0, the pH range which corresponds to the plateau region of the shoulder of the pH–rate profile where the maximum inhibition obtainable with threonine is approximately 65%. A difference curve derived from the two pH–rate profiles is shown in the inset of Figure 2.

Patte *et al.* (1963) have reported a potassium ion activation of homoserine dehydrogenase I isolated from *E. coli* K 12 Hfr H. As demonstrated in Figure 3A, we have also found a potassium ion requirement for the enzyme isolated from *E. coli* K 12λ. Furthermore, the data of Figure 3A suggest that potassium ion is an essential activator of the enzyme at pH 9 in both the presence of and virtual absence of L-threonine. The sigmoid character of the potassium ion activation curves also suggests the existence of a cooperative homotropic interaction of potassium ion binding sites on the enzyme. The points in Figure 3A represent the experimentally determined values and the solid curves represent the theoretical curves calculated from eq 1, the derivation of which will be discussed in a later section. It is also apparent from Figure 3A that a K^+ concentration of 400 mM essentially saturates the enzyme even at high concentrations of L-threonine; therefore, unless otherwise stated, all subsequent experiments were carried out in 400 mM KCl. In Figure 3B, the data of Figure 3A are shown as double-reciprocal plots, $1/v$ *vs.* $1/[K^+]^2$, with the points representing the experimentally determined values and the solid lines representing the theoretical curves calculated from eq 1. Both plots appear linear over a wide range in potassium ion concentration, suggesting the involvement of two or more potassium ions in the activation of the enzyme. Further support for the hypothesis that at least two potassium ions are involved in the activation process at pH 9 is provided by Hill plots (Brown and Hill, 1922) of the data of Figure 3A. A linear regression analysis of a Hill plot, $\log v/(V_{max} - v)$ *vs.* $\log [K^+]$, of the data of Figure 3A at 33 μM L-threonine indicates an n value of 1.83 and a correlation coefficient of 0.993. A similar analysis of the data at 5.03 mM L-threonine indicates an n value of 1.91 and a correlation coefficient of 0.990. The results of preliminary experiments indicate that ammonium ions also activate the enzyme but that sodium ions do not. On the other hand, sodium ions strongly antagonize the activation by potassium ions as reported by Patte *et al.* (1963).

Double-reciprocal plots, $1/v$ *vs.* 1/[L-homoserine] at three concentrations of $NADP^+$ and $1/v$ *vs.* $1/[NADP^+]$ at three concentrations of L-homoserine, are presented in Figures 4 and 5,

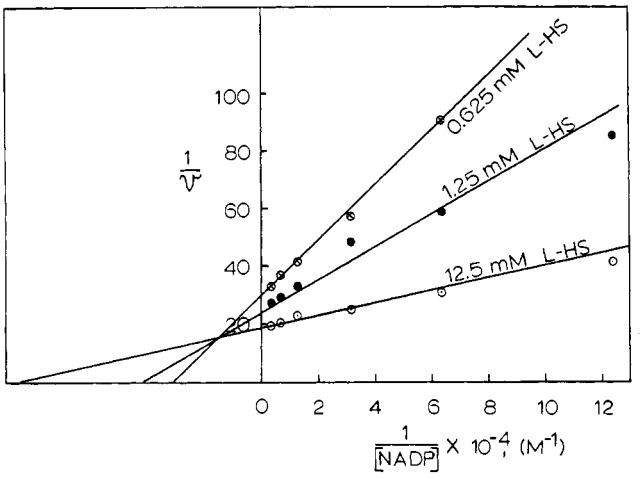

FIGURE 5: Double-reciprocal plots of initial reaction velocity *vs.* $NADP^+$ concentration at three different initial concentrations of homoserine. Initial assay conditions: 0.1 M Tris (pH 9.1), 0.4 M KCl, 33 μM L-threonine and either 25 mM DL-homoserine (⊙), 2.5 mM DL-homoserine (●), or 1.25 mM DL-homoserine (⊗). Initial velocity expressed as Δ absorbance per minute at 340 mμ. Solid lines: theoretical curves calculated from eq 1.

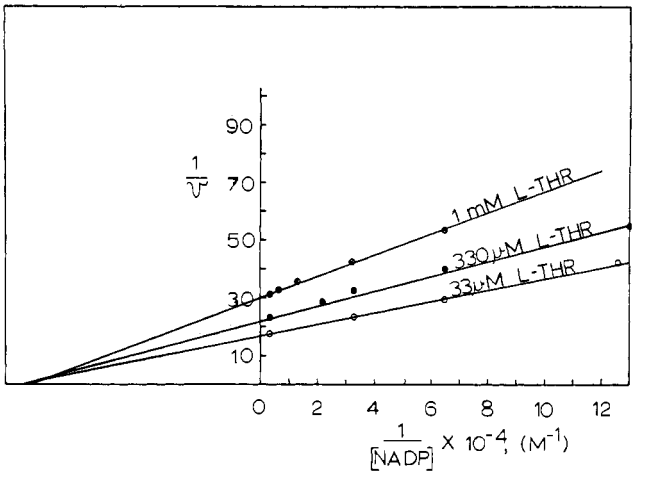

FIGURE 7: Double-reciprocal plots of the initial reaction velocity *vs.* $NADP^+$ concentration at three different L-threonine concentrations. Initial assay conditions: 0.1 M Tris-HCl (pH 8.9), 0.4 M KCl, and either 25 mM DL-homoserine plus 33 μM L-threonine (⊙), 50 mM DL-homoserine plus 330 μM L-threonine (●), or 50 mM DL-homoserine plus 1.0 mM L-threonine (⊗). Initial velocity expressed as Δ absorbance per minute at 340 mμ. Solid lines: theoretical curves calculated from eq 1.

respectively. The points in each figure represent the experimentally determined values and the solid lines are the theoretical curves calculated from eq 1. All of the double-reciprocal plots in these two figures appear to be linear, even when the concentration of the second substrate is maintained at a less than saturating concentration.

The effect of the inhibitor, L-threonine, on the initial velocity of the reaction at pH 8.90 and at near-saturating concentrations of K^+, $NADP^+$, and L-homoserine is depicted in Figure 6, with the points representing the experimentally determined values and the solid curve the theoretical curve calculated according to eq 1. Although it has been reported that homoserine dehydrogenase I from *E. coli* K 12 Hfr H displays a sigmoid saturation curve with respect to L-threonine (Patte *et al.*, 1966), our data on the enzyme from *E. coli* K 12λ do not indicate a sigmoid saturation curve. Cunningham *et al.* (1968) have also reported that the effect of L-threonine on homoserine dehydrogenase isolated from *E. coli* 9723 is consistent with the independent interaction of threonine at a single regulatory site. Furthermore, as indicated in Figures 7 and 8, a significant concentration of L-threonine does not induce a detectable nonlinearity in the plots of either $1/v$ *vs.* $1/[NADP^+]$ or $1/v$ *vs.* 1/[L-homoserine]. Thus, the presence of the inhibitor does not result in the appearance of any demonstrable homotropic interactions of either the substrate or the cofactor. The solid curves of Figures 7 and 8 again represent the

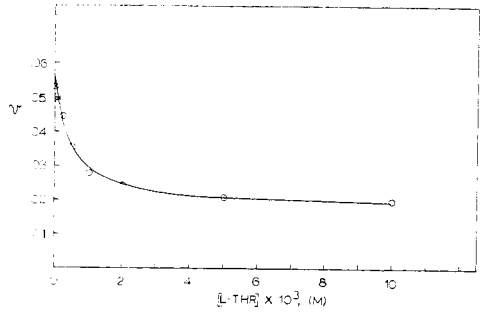

FIGURE 6: Effect of L-threonine concentration on the initial reaction velocity. Initial assay conditions: 0.1 M Tris-HCl (pH 8.9), 0.4 M KCl, 25 mM DL-homoserine, and 309 μM $NADP^+$. Initial velocity expressed as Δ absorbance per minute at 340 mμ. Solid line: theoretical curve calculated from eq 1.

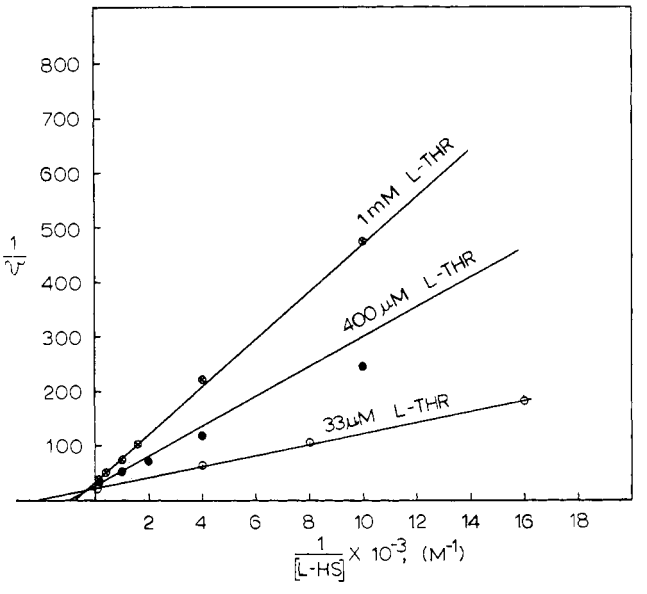

FIGURE 8: Double-reciprocal plots of the initial reaction velocity *vs.* homoserine concentration at three different L-threonine concentrations. Initial assay conditions: 0.1 M Tris-HCl (pH 8.8), 0.4 M KCl, 309 μM $NADP^+$, and either 33 μM L-threonine (⊙), 400 μM L-threonine (●), or 1.0 mM L-threonine (⊗). Initial velocity expressed as Δ absorbance per minute at 340 mμ. Solid lines: theoretical curves calculated from eq 1.

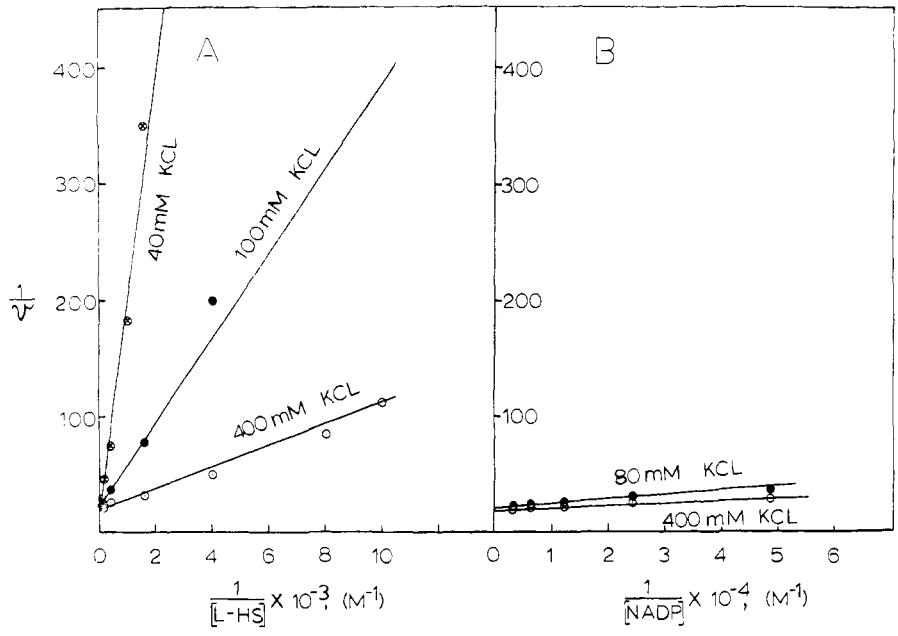

FIGURE 9: Double-reciprocal plots of the initial reaction velocity. (A) Versus homoserine concentration at three different potassium ion concentrations. Initial assay conditions: 0.1 M Tris-HCl (pH 8.85), 309 μM $NADP^+$, 33 μM L-threonine, and either 400 mM KCl (⊙), 100 mM KCl (●), or 40 mM KCl (⊗). (B) Versus $NADP^+$ concentration at two different potassium ion concentrations. Initial assay conditions: 0.1 M Tris-HCl (pH 8.85), 25 mM DL-homoserine, 42 μM L-threonine, and either 400 mM KCl (⊙), or 80 mM KCl (●). Initial reaction velocities in parts A and B are expressed as Δ absorbance per minute at 340 mμ. Solid lines in parts A and B are theoretical curves calculated from eq 1.

TABLE II: Kinetic Parameters of the Homoserine Dehydrogenase Catalyzed Reaction of L-Homoserine with $NADP^+$.

Source of Data	Experimental Conditions	V_{max}' ± SE (ΔA_{340}/min × 10^4)	K_m' ± SE (M²)
Figure 3[a]	33 μM L-threonine, 310 μM $NADP^+$, 12.5 mM L-homoserine	479 ± 11	0.001411 ± 0.000146
	5.03 mM L-threonine, 310 μM $NADP^+$, 12.5 mM L-homoserine	185 ± 4	0.00946 ± 0.00090
			(μM)
Figure 4	309 μM $NADP^+$, 33 μM L-threonine	565 ± 26	570 ± 80
	25 μM $NADP^+$, 33 μM L-threonine	361 ± 7	1070 ± 70
	12.5 μM $NADP^+$, 33 μM L-threonine	275 ± 6	1370 ± 110
Figure 5	12.5 mM L-homoserine, 33 μM L-threonine	517 ± 17	9.6 ± 1.4
	1.25 mM L-homoserine, 33 μM L-threonine	379 ± 11	19.6 ± 1.7
	0.625 mM L-homoserine, 33 μM L-threonine	329 ± 6	28.9 ± 1.6
Figure 7	33 μM L-threonine, 12.5 mM L-homoserine	594 ± 10	11.8 ± 0.6
	330 μM L-threonine, 25 mM L-homoserine	432 ± 7	11.3 ± 0.6
	1 mM L-threonine, 25 mM L-homoserine	329 ± 2	12.0 ± 0.3
Figure 8	33 μM L-threonine, 309 μM $NADP^+$	463 ± 4	506 ± 16
	400 μM L-threonine, 309 μM $NADP^+$	347 ± 4	765 ± 22
	1 mM L-threonine, 309 μM $NADP^+$	324 ± 4	1549 ± 58
Figure 9A	400 mM KCl, 33 μM L-threonine	517 ± 16	373 ± 40
	100 mM KCl, 33 μM L-threonine	535 ± 9	2290 ± 130
	40 mM KCl, 33 μM L-threonine	442 ± 26	5530 ± 800
Figure 9B	400 mM KCl, 42 μM L-threonine	527 ± 12	11.1 ± 1.8
	80 mM KCl, 42 μM L-threonine	485 ± 10	16.5 ± 1.8

[a] The data of Figure 3 were analyzed by the Wilkinson method by assuming that two potassium ions activate the enzyme with infinite cooperativity, *i.e.*, $v = V_{max}'[K^+]^2/(K_m' + [K^+]^2)$.

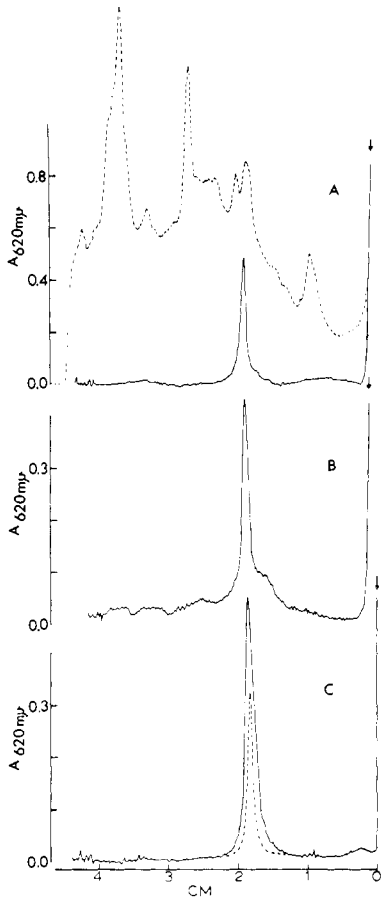

FIGURE 10: Disc gel electrophoresis of homoserine dehydrogenase preparations. Electrophoresis, staining, and scanning carried out as described in Methods. (A) A 435-μg sample of fraction II (second 30–45% $(NH_4)_2SO_4$ fraction) stained for protein (- - - - -) and homoserine dehydrogenase activity (———). (B) An 11-μg sample of fraction IV (Sepharose fraction) stained for protein. (C) An 11-μg sample of fraction IV (Sepharose fraction) stained for homoserine dehydrogenase activity with a substrate solution containing no threonine (———) and with a substrate solution containing 20 mM L-threonine (- - - - -). The ratio of the homoserine dehydrogenase activities in the samples applied to the gel column was fraction II/fraction IV = 1.2, as determined by the standard assay procedure. With the exception of the threonine concentration, the staining procedure for detecting homoserine dehydrogenase activity was identical in all experiments. The arrows indicate the interface between the large and small pore gels; the abscissa represents the gel column length in centimeters.

theoretical curves calculated from eq 1 and are in reasonable agreement with the experimental data represented by the points. The data of Figures 7 and 8 also indicate that threonine produces a noncompetitive-type inhibition with respect to $NADP^+$ and a mixed-type inhibition with respect to homoserine. Thus, the enzyme of this study would appear to differ somewhat from the enzyme of *E. coli* K 12 Hfr H, for which a noncompetitive-type inhibition with respect to homoserine has been reported (Patte *et al.*, 1963).

Plots of $1/v$ *vs.* 1/[L-homoserine] and $1/v$ *vs.* 1/[$NADP^+$] at several different potassium ion concentrations are presented in Figure 9A,B. It can be seen from these figures that the plots remain linear even in the presence of less than saturating concentrations of K^+ and that the theoretical curves are in reasonable agreement with the experimental points. Furthermore, the data of Figure 9A suggest a common intercept on the $1/v$ axis at the three different potassium ion concentrations employed.

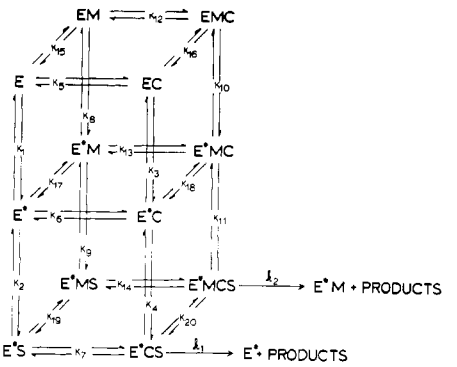

FIGURE 11: Tentative model for homoserine dehydrogenase. E is free enzyme, M is L-threonine, C is $NADP^+$, E* is enzyme fully activated by potassium, and S is L-homoserine. See text for details.

The preceding kinetic data, although presented graphically in the double-reciprocal forms of Lineweaver and Burk (1934), were analyzed by the statistical method described by Wilkinson (1961). The apparent maximum velocities, V_{max}', and Michaelis constants, K_m', determined by this statistical treatment are listed in Table II. The data of Figure 3 were anaylzed by the Wilkinson method by assuming that two potassium ions activate the enzyme with infinite cooperativity, *i.e.*, $v = V_{max}'[K^+]^2/(K_m' + [K^+]^2)$.

The specific activity of fraction II, the enzyme preparation employed in the preceding kinetic studies, was approximately 7.5-fold greater than the specific activity of the crude extract isolated after sonic disruption of the *E. coli*. More recently, fraction IV, which represents a purification of approximately 350-fold relative to the crude extract, has been obtained. These two fractions, fraction II and fraction IV, have been analyzed by disc electrophoresis and the results are presented in Figure 10. It is apparent that only one band in each preparation stains for homoserine dehydrogenase activity and that the homoserine dehydrogenase activity coincides with the major protein band in the gel containing the more highly purified preparation. Furthermore, it has been found that L-threonine inhibits the enzymatic activity of fraction IV to exactly the same extent that it inhibits the enzymatic activity of fraction II. Thus, additional purification does not appear to alter the enzyme's sensitivity to threonine.

Discussion

The interesting kinetic properties of homoserine dehydrogenase I led us to search for a kinetic model which would be consistent with the experimental data. Thus far, the simplest model which we have found to be consistent with all of the data is the one presented in Figure 11, where E is free enzyme, E* is enzyme fully activated by K^+, C is $NADP^+$, S is L-homoserine, M is L-threonine, and K_1, K_2, ... K_{20} are equilibrium constants of the various equilibria shown, written as dissociation constants, *i.e.*, $K_1 = [E][K^+]^2/[E^*]$, $K_2 = [E^*][S]/[E^*S]$, etc. The front plane represents the activation of the enzyme by K^+ (assumed to involve two K^+ binding sites dis-

$$v = \frac{V + \frac{[M]}{K_{20}}V'}{\left(\frac{K_3K_4K_5}{[K^+]^2[S][C]} + \frac{K_3K_4}{[K^+]^2[S]} + \frac{K_4K_6}{[S][C]} + \frac{K_4}{[S]} + \frac{K_7}{[C]} + \frac{K_4K_6K_8[M]}{K_{17}[S][C][K^+]^2} + \frac{K_4K_6[M]}{K_{17}[S][C]} + \frac{K_4K_{10}[M]}{K_{18}[S][K^+]^2} + \frac{K_4[M]}{K_{18}[S]} + \frac{K_7[M]}{K_{19}[C]} + \frac{[M]}{K_{20}} + 1\right)} \quad (1)$$

playing essentially infinite cooperativity) and the formation of enzyme–substrate complexes in the absence of threonine. The rear plane represents similar pathways for the enzyme when it contains bound threonine. Thus, in principle, the equilibria of the front plane (K_1–K_7) and the equilibria of the rear plane (K_8–K_{14}) may be investigated independently through studies carried out in the absence of threonine and at saturating concentrations of threonine, respectively. Proceeding from the compounds or complexes in the upper plane to those in the middle plane involves the activation by K^+; proceeding from the complexes in the middle plane to those in the lower plane involves the addition of homoserine; proceeding from the compounds or complexes in the plane to the left to those in the plane to the right involves addition of $NADP^+$. The salient features of the model are (1) both the activated enzyme–substrate complex, E*CS, and the activated enzyme–substrate–threonine complex, E*MCS, are capable of forming products but at different rates ($k_2 < k_1$), (2) activation of the enzyme by the addition of K^+ must proceed homoserine addition, and (3) the activation by K^+ involves two K^+ binding sites displaying essentially infinite cooperativity. The experimental basis for incorporating the first of the above features into the model is apparent from the data given in Figure 6 which indicate that total inhibition by L-threonine is not obtainable at pH 8.9; the experimental basis for incorporating the second feature is to be found in the data of Figure 3A which demonstrate the essential nature of the activation by potassium ions and in the data of Figure 9A which suggest a common intercept on the $1/v$ axis at three different concentrations of potassium ions; the experimental basis for incorporating the third feature appears in Figure 3B, in which a plot of $1/v$ *vs.* $1/[K^+]^2$ is observed to be reasonably linear over a wide range in potassium ion concentration.

A rapid equilibrium treatment of the model depicted in Figure 11 yields eq 1, an expression for the initial velocity, where v is the initial velocity, V is the maximum velocity in the absence of threonine ($V = k_1[E_0]$, where $[E_0]$ is the total enzyme concentration and k_1 is the rate constant for the breakdown of the E*CS complex to form products), V' is the maximum velocity in the presence of a saturating concentration of threonine ($V' = k_2[E_0]$, where $[E_0]$ is the total enzyme concentration and k_2 is the rate constant for the breakdown of the E*MCS complex to form products), and K_3, K_4, ... K_{20} are the dissociation constants. Of the 20 dissociation constants represented in Figure 11, 11 are independent and appear in eq 1; the remaining 9 dissociation constants are dependent and do not appear in the equation.

In the presence of a saturating concentration of K^+, eq 1 may be simplified by neglecting those terms involving $[K^+]$ in the denominator, yielding eq 2. If it is assumed as a working hypothesis that eq 2 correctly describes the homoserine dehydrogenase reaction at a saturating concentration of K^+, it can be shown from the data of Figure 7 and Table II that K_{19}

$$v = \frac{V + \frac{[M]}{K_{20}}V'}{\frac{K_4K_6}{[S][C]} + \frac{K_4}{[S]} + \frac{K_7}{[C]} + \frac{K_4K_6[M]}{K_{17}[S][C]} + \frac{K_4[M]}{K_{18}[S]} + \frac{K_7[M]}{K_{19}[C]} + \frac{[M]}{K_{20}} + 1} \quad (2)$$

must equal K_{20} since the intercept on the $1/[NADP^+]$ axis is independent of the concentration of threonine at two different saturating concentrations of homoserine.[1] Thus a value for K_7 can be obtained from the intercept on the $1/[NADP^+]$ axis in Figure 7, and values for K_{20} and K_{19} can be estimated algebraically from both the intercepts on the $1/v$ axis and from the slopes of the plots. These values for K_7 and K_{20}, as well as values obtained from other data presented in Table II, are given in Table III. As a consequence of the model, K_7 must equal K_{14} if $K_{19} = K_{20}$; therefore, the affinity of E*S for threonine is not altered by the binding of $NADP^+$, and the affinity of E*S for $NADP^+$ is unchanged by the binding of threonine.

In the absence of M, eq 2 reduces to eq 3. From the data of

$$v = \frac{V}{\frac{K_4K_6}{[S][C]} + \frac{K_4}{[S]} + \frac{K_7}{[C]} + 1} \quad (3)$$

Figures 4, 5, 8, and 9 and Table II, the values for K_4 and K_6 which are presented in Table III can be estimated algebraically. These values were obtained by assuming that the 33 μM L-threonine present in these experiments was not significant, *i.e.*, $[M]=0$. Since this assumption is not strictly valid, the estimated values for K_4 which are presented in Table III should be slightly larger than the true value.

The only equilibrium constants in eq 2 which remain undetermined are K_{17} and K_{18}. From eq 2, it is apparent that a

[1] The intercept, I, on the $1/[NADP^+]$ axis is

$$-I = \frac{\left(\frac{K_4}{[S]} + \frac{K_4[M]}{K_{18}[S]} + \frac{[M]}{K_{20}} + 1\right)}{\left(\frac{K_4K_6}{[S]} + \frac{K_4K_6[M]}{K_{17}[S]} + \frac{K_7[M]}{K_{19}} + K_7\right)}$$

If I is independent of [S], those terms involving [S] must be negligible with respect to the other terms; therefore

$$-I = \frac{\left(\frac{[M]}{K_{20}} + 1\right)}{K_7\left(\frac{[M]}{K_{19}} + 1\right)}$$

Furthermore, if I is independent of [M], K_{19} must equal K_{20}, and, therefore, $-I = 1/K_7$.

TABLE III: Dissociation Constant Values.

K	Estimated Values (M^2)	Av Value (M^2)	Theor Value (M^2)
$K_1 = K_3$	0.032	0.032	0.025
$K_8 = K_{10}$	0.094	0.094	0.10
	(M)	(M)	(M)
K_4	4.7×10^{-4}, 4.7×10^{-4}, 5.4×10^{-4} 4.5×10^{-4}, 3.6×10^{-4}, 3.7×10^{-4} 5.1×10^{-4}	4.5×10^{-4}	3×10^{-4}
K_7	1.2×10^{-5}, 1.1×10^{-5}, 1.2×10^{-5}	1.1×10^{-5}	1×10^{-5}
$K_{17} = K_{18}$	1.6×10^{-4}, 2.0×10^{-4}	1.8×10^{-4}	1.7×10^{-4}
$K_{19} = K_{20}$	5.2×10^{-4}, 5.1×10^{-4}, 5.3×10^{-4}	5.2×10^{-4}	5.2×10^{-4}
$K_5 = K_6$	6.5×10^{-5}, 6.2×10^{-5}, 6.5×10^{-5}	6.4×10^{-5}	6.5×10^{-5}

plot of $(V + [M]V'/K_{20})/v$ *vs.* [M] should be linear with a slope equal to

$$\frac{K_4K_6}{K_{17}[S][C]} + \frac{K_4}{K_{18}[S]} + \frac{K_7}{K_{19}[C]} + \frac{1}{K_{20}}$$

Two such plots, one at a near-saturating concentration of L-homoserine and one at a low concentration of L-homoserine, are presented in Figure 12. If it is assumed that $K_{17} = K_{18}$, then the values of K_{17} and K_{18} can be estimated algebraically from the data of Figure 12 by employing the average values of K_4, K_6, K_7, K_{19}, and K_{20} given in Table III. The only basis for the assumption that $K_{17} = K_{18}$ (*i.e.*, that the affinities of E* and E*C for threonine are identical) is by analogy with the affinities of E*S and E*CS for threonine, which were found to be equal ($K_{19} = K_{20}$). As a consequence of the model, K_6 must equal K_{13} if K_{17} is equal to K_{18}. The values of K_{17} and K_{18} determined in this manner are presented in Table III.

Equation 1 still contains 4 as yet undetermined constants, K_3, K_5, K_8, and K_{10}. It can be seen from eq 1 that the slope of the $1/v$ *vs.* $1/[K^+]^2$ plots of Figure 3B should be

$$\text{slope} = \left(\frac{1}{V + \frac{[M]}{K_{20}}V'}\right) \times \left(\frac{K_4}{[S]}\right)\left(\frac{K_3K_5}{[C]} + K_3 + \frac{K_6K_8[M]}{K_{17}[C]} + \frac{K_{10}[M]}{K_{18}}\right) \quad (4)$$

If it is assumed that the affinity of the enzyme for $NADP^+$ is independent of the binding of K^+ (*i.e.*, $K_5 = K_6$), that the affinity of the enzyme for K^+ is independent of the binding of $NADP^+$ (*i.e.*, $K_1 = K_3$ and $K_8 = K_{10}$), and that a threonine concentration of 33 μM is negligible, values for K_1, K_3, K_8, and K_{10} may be estimated algebraically from the data of Figure 3B by employing the average values given in Table III for the previously determined constants K_4, K_6, K_{17}, K_{18}, and K_{20}. The values of K_1, K_3, K_8, and K_{10} estimated in this manner are given in Table III. The only experimental evidence suggesting that the assumptions $K_5 = K_6$, $K_1 = K_3$, and $K_8 = K_{10}$ might be valid is the observation that the K_m' for $NADP^+$ appears relatively insensitive to the concentration of K^+ (Figure 9B and Table II). The assumption that a concentration of 33 μM threonine is negligible is again not strictly valid, however, the error that this assumption might introduce into K_3 should be compensated by the error introduced by this same assumption in the value determined for K_4.

It remains to be shown that eq 1 and a single set of dissociation constants with values in the ranges of those reported in Table III will yield calculated initial velocities in reasonable agreement with the observed velocities. That this is indeed the case can be seen in Figures 3A,B, 4, 5, 6, 7, 8, 9A,B, and 12 in which the solid curves represent values calculated by eq 1 and the individual points represent the experimental data. The dissociation constant values employed in these calculations are listed in the final column of Table III and are labeled theo-

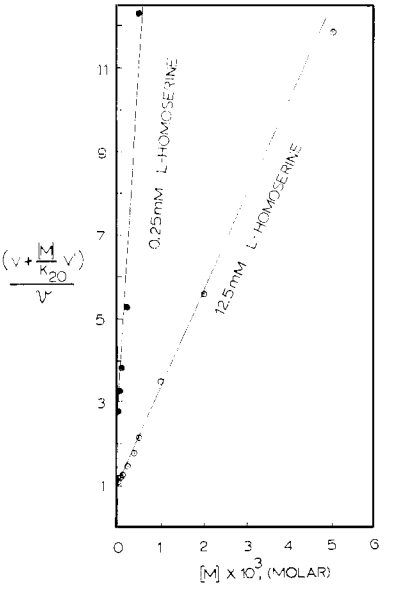

FIGURE 12: Plots of $(V + [M]V'/K_{20})/v$ *vs.* concentration of M, where M is L-threonine, at two different concentrations of homoserine. Assay conditions described in legend of Figure 6. Solid lines theoretical curves calculated from eq 1.

retical values. The theoretical values of the dissociation constants were obtained by adjusting the average estimated values listed in Table III until a reasonable agreement was achieved between all of the experimental data and the corresponding data calculated *via* eq 1. The largest adjustment made was to decrease the average estimated value of K_4 by one-third; however, in view of the assumptions made in arriving at the estimated value of K_4, the necessity for this adjustment was expected. Although it is very probable that minor adjustments in the theoretical values for the dissociation constants could be made which would result in an even better fit of the calculated data to the experimental data, the agreement achieved when the theoretical values listed in Table III are employed appears to be sufficient to justify the conclusion that the model presented in Figure 11 is consistent with the experimental data.

A number of objections to the proposed model can be raised, the first of which might be the rapid equilibrium assumption. However, the fact that threonine, a noncompetitive inhibitor, does not induce any detectable nonlinearity into the double-reciprocal plots of the data supports the assumption that the system is functioning at or close to quasi-equilibrium (Walter, 1965). It might also be argued that the enzyme preparation contains two species of homoserine dehydrogenase, one sensitive to threonine and one insensitive to threonine, thus explaining the inability of threonine to produce a complete inhibition of the enzymatic activity, as well as explaining the unusual pH–rate profile of the enzyme in the presence of low concentrations of threonine (Figure 2). However, on the basis of a number of other observations, this possibility would appear to be very unlikely. For example, no preparation of the *E. coli* enzyme examined thus far can be completely inhibited at pH 9 by threonine (Patte *et al.*, 1963; Cunningham *et al.*, 1968). Although the particular enzyme preparation used in the present kinetic investigation was not a highly purified preparation, it displayed a single, sharp, well-defined band of homoserine dehydrogenase activity on disc electrophoresis (Figure 10). Furthermore, fraction IV, a very highly purified preparation, is inhibited by threonine to the same extent as the fraction II preparation used in the kinetic studies (Figure 10). Thus, if there are two species of the enzyme present in the preparation employed, they are not resolvable by the battery of purification procedures used, including disc electrophoresis. Other observations also support the conclusion that all of the enzyme molecules interact with threonine. For example, it has been found that threonine protects all of the enzymatic activity from destruction by mild heat treatment and that threonine produces an approximate doubling of the apparent molecular weight of the enzyme (Ogilvie and Sightler, 1968). In addition, if there were two species of the enzyme, the data of Figure 7 would require that they both possess identical Michaelis constants for $NADP^+$ and Figures 3A,B would require that they both show a similar type of essential activation by K^+ at pH 9.

The explanation for the unusual pH–rate profile shown in Figure 2 is unknown. Extrapolation of the data presented suggests that the activity of the enzyme may become independent of the concentration of threonine in the vicinity of pH 10; however, the incompleteness of the data in this pH region prohibits the forming of any definite conclusions. If the two curves of Figure 2 do indeed become coincident in the higher pH range, a simple explanation would be that the enzyme preparation contains two species, one species completely inhibitable by threonine and possessing a pH–rate profile identical with that presented in the inset of the figure and the other species completely insensitive to threonine and possessing a pH–rate profile identical with that shown for the enzyme in the presence of 5 mM threonine. For the reasons stated in the preceding paragraph, this explanation would appear unlikely unless the two different species are closely associated to form a complex. Other explanations invoking pH-dependent changes in the conformation of the enzyme are plausible but cannot be established by the existing data.

The amino acid composition of the homoserine dehydrogenase I–aspartokinase I complex of *E. coli* K 12 Hfr H has recently been determined (Truffa-Bachi *et al.*, 1968); however, little is known about the molecular structure of this interesting enzyme. At pH 7.6, threonine produces an approximate doubling of the apparent molecular weight of the *E. coli* K 12 enzyme employed in this study (Ogilvie and Sightler, 1968); however, the threonine-induced aggregation of the enzyme may not be directly involved in the mechanism of the threonine inhibition of the enzyme (Barber and Bright, 1968). Until the molecular structure of this enzyme is better understood, attempts to rationalize aspects of the kinetic model proposed in Figure 11 in terms of mechanisms at the molecular level are not likely to be very productive.

Although the model presented in Figure 11 appears to be consistent with the experimental data obtained thus far, other models may exist which are also compatible with the data. Direct measurements of the various dissociation constants proposed in the model will be attempted as soon as a sufficient quantity of the homogeneous enzyme preparation is available. A comparison of the directly determined values for the dissociation constants with the kinetically determined values should allow one to assess the validity of the proposed model.

References

Atkinson, D. E., Hathaway, J. A., and Smith, E. C. (1965), *J. Biol. Chem. 240*, 2682.

Black, S., and Wright, N. G. (1955), *J. Biol. Chem. 213*, 39.

Barber, E. D., and Bright, H. J. (1968), *Proc. Natl. Acad. Sci. U. S. 60*, 1363.

Brown, W. E. L., and Hill, A. V. (1922), *Proc. Roy. Soc. (London) B94*, 297.

Changeux, J.-P., and Rubin, M. M. (1968), *Biochemistry 7*, 553.

Cohen, G. N., and Rickenberg, H. V. (1956), *Ann. Inst. Pasteur 91*, 693.

Cunningham, G. N., Maul, S. B., and Shive, W. (1968), *Biochem. Biophys. Res. Commun.* 30, 159.

Datta, P., and Gest, H. (1965), *J. Biol. Chem. 240*, 3023.

Davis, B. J. (1964), *Ann. N. Y. Acad. Sci. 121*, 404.

Davis, C. H., Schliselfeld, L. H., Wolf, D. P., Leavitt, C. A., and Krebs, E. G. (1967), *J. Biol. Chem. 242*, 4824.

Evans, H. J., and Nason, A. (1953), *Plant Physiol. 28*, 233.

Ferdinand, W. (1966), *Biochem. J. 98*, 278.

Frieden, C. (1963), *J. Biol. Chem. 238*, 3286.

Frieden, C. (1964), *J. Biol. Chem. 239*, 3522.

Frieden, C. (1967), *J. Biol. Chem. 242*, 4045.

Frieden, C., and Colman, R. F. (1967), *J. Biol. Chem. 242*, 1705 (1967).

Kirschner, K., Eigen, M., Bittman, R., and Voigt, B. (1966),

Proc. Natl. Acad. Sci. U. S. 56, 1661.
Koshland, D. E., Nemethy, G., and Filmer, D. (1966), *Biochemistry 5*, 365.
Lineweaver, H., and Burk, D. (1934), *J. Am. Chem. Soc. 56*, 658.
Monod, J., Wyman, J., and Changeux, J.-P. (1965), *J. Mol. Biol. 12*, 88.
Ogilvie, J. W., and Sightler, J. H. (1968), *Biophys. J. 8*, A-90.
Patte, J. C., LeBras, G., Loviny, T., and Cohen, G. N. (1963), *Biochim. Biophys. Acta 67*, 16.
Patte, J. C., Truffa-Bachi, P., and Cohen, G. N. (1966), *Biochim Biophys. Acta 128*, 426.
Peterson, E. A., and Sober, H. A. (1956), *J. Am. Chem. Soc. 78*, 751.
Rabin, B. R. (1967), *Biochem. J. 102*, 22C.
Sanwal, B. D., Stachow, C. S., and Cook, R. A. (1965), *Biochemistry 4*, 410.
Sweeny, J. R., and Fisher, J. R. (1968), *Biochemistry 7*, 561.
Truffa-Bachi, P., van Rapenbusch, R., Janin, J., Gros, C., and Cohen, G. N. (1968), *European J. Biochem. 5*, 73.
Walter, C. (1965), Steady-State Applications in Enzyme Kinetics, New York, N. Y., Ronald, pp 175–179.
Warburg, O., and Christian, W. (1941), *Biochem. Z. 310*, 384.
Wilkinson, G. N. (1961), *Biochem. J. 80*, 324.
Zamenhof, S. (1957), *Methods Enzymol. 3*, 702.

Structure of the Cell Wall Peptidoglycan of *Lactobacillus casei* RO94*

K. D. Hungerer,† J. Fleck,‡ and D. J. Tipper§

ABSTRACT: The cell wall peptidoglycan of *Lactobacillus casei* RO94 contains almost equimolar proportions of D-glutamic acid, D-alanine, L-alanine, L-lysine, D-aspartic acid, *N*-acetylmuramic acid, *N*-acetylglucosamine, and two molar proportions of ammonia. Glycan chains of alternating, β-1,4-linked residues of *N*-acetylglucosamine and *N*-acetylmuramic acid have an average chain length of about ten disaccharides and are substituted on every muramic acid residue by the pentapeptide N^{α}-(L-alanyl-D-isoglutaminyl)-N^{ϵ}-(D-isoasparaginyl)-L-lysyl-D-alanine, randomly cross-linked between D-alanine and D-isoasparagine to the extent of 55%. The *Myxobacter* AL-1 enzyme hydrolyses all of the D-alanyl-D-isoasparaginyl linkages and most of the *N*-acetylmuramyl-L-alanine linkages in the peptidoglycan resulting in the production of hexosamine-free peptide monomers and of an almost peptide-free complex of glycan and group C-specific polysaccharide. The group C-specific polysaccharide is linked to the glycan by highly acid-labile phosphodiester linkages and hydrolysis of the complex gives rise to muramic acid 6-phosphate.

The cell walls of *Lactobacillus casei*, like those of many gram-positive bacteria, contain D-glutamic acid, L-lysine, L-alanine, and D-alanine (Ikawa and Snell, 1960). These amino acids form the peptide component of UDP-*N*-acetylmuramyl-L-alanyl-D-isoglutamyl-L-lysyl-D-alanyl-D-alanine which, together with variants in which L-alanine and lysine are replaced by other amino acids, is probably a biosynthetic precursor of all bacterial cell wall peptidoglycans (*cf.* Ghuysen *et al.*, 1968). The peptide moiety, lacking its C-terminal D-alanine residue, is found intact in the cell walls of several bacteria (Muñoz *et al.*, 1966; Jarvis and Strominger, 1967) and, as will be shown, not unexpectedly occurs also in the cell walls of *L. casei*.

Peptidoglycans containing this tetrapeptide are all cross-linked between D-alanine and the ε-amino group of lysine in a neighboring peptide, but differ in the nature of this link, *e.g.*, a direct linkage occurs in *Micrococcus lysodeikticus* (Petit *et al.*, 1966), pentaglycine with a variable extent of replacement by L-serine occurs in staphylococci (Tipper and Berman, 1969) and peptides of L-alanine and L-threonine occur in *Micrococcoccus roseus* (Petit *et al.*, 1966). *L. casei* cell walls contain aspartic acid (Cummins and Harris, 1956) and acid hydrolysis of these walls yields N^{ϵ}-(aminosuccinoyl)-L-lysine, a compound which is very resistant to acid hydrolysis and which is derived during hydrolysis from N^{ϵ}-(α- or β-aspartyl)-L-lysine (Swallow and Abraham, 1958). Thus drastic and prolonged hydrolysis is required if a reasonable yield of aspartic acid is to be obtained from these cell walls, and this leads to considerable racemization (Ikawa, 1964) and some destruction (see below) of the aspartic acid. Nevertheless, it is probable that at least 90% of the aspartic acid of the peptidoglycan has the D configuration (Ikawa, 1964). N^{ϵ}-(α- or β-D-aspartyl)-L-lysine therefore

* From the Department of Pharmacology, University of Wisconsin Medical School, Madison, Wisconsin 53706. *Received April 7, 1969.* This investigation was supported by a U. S. Public Health Service research grant (HD 02972), a Career Research Development award (GM 38652), and a National Science Foundation research grant (GB-6416). A preliminary report of these results has been published (Hungerer, 1968).

† Present address: Max-Planck Institut für Immunobiologie, Freiburg, Germany.
‡ Present address: Institut de Bacteriologie, Strasbourg, France.
§ To whom inquiries should be addressed for reprints.